

Supporting Information

Two-Bond ^{13}C - ^{13}C Spin-Coupling Constants in Saccharides: Dependencies on Exocyclic Hydroxyl Group Conformation

Jieye Lin,¹ Reagan Meredith,¹ Allen Oliver,² Ian Carmichael,³ and Anthony S. Serianni^{1*}

¹Department of Chemistry and Biochemistry, ²Molecular Structure Facility, and the ³Radiation Laboratory, University of Notre Dame, Notre Dame, IN 46556-5670 USA

Table of Contents

1. Chemical synthesis, solution and solid-state NMR spectra, and X-ray crystallography of 6 ^{1,3}	S2–S3
2. Chemical synthesis, solution and solid-state NMR spectra, and X-ray crystallography of 7 ^{1,3}	S4–S5
3. Chemical synthesis, solution and solid-state NMR spectra, and X-ray crystallography of 8 ^{1,3}	S6–S10
4. Chemical synthesis, solution and solid-state NMR spectra, and X-ray crystallography of 8 ^{1',3'}	S11–S13
5. Chemical synthesis, solution and solid-state NMR spectra, and X-ray crystallography of 9 ^{1,3}	S14–S15
6. Chemical synthesis, solution and solid-state NMR spectra, and X-ray crystallography of 9 ^{1',3'}	S16–S17
7. X-ray crystallography of 1 ^{1,3}	S17
8. Effect of solid-state NMR sample preparation on the crystal structure of 8	S18–21
9. Table S7. Fitting statistics from solid-state ^{13}C NMR determinations of $^2J_{\text{CCC}}$ values in crystalline 6 ^{1,3} , 7 ^{1,3} , 8 ^{1,3} , 8 ^{1',3'} , 9 ^{1,3} and 9 ^{1',3'}	S22
10. Figure S15. Plots of S/S_0 vs τ to determine $^2J_{\text{C1,C3}}$ or $^2J_{\text{C1',C3'}}$ in 6 ^{1,3} , 7 ^{1,3} , 8 ^{1,3} , 8 ^{1',3'} , 9 ^{1,3} and 9 ^{1',3'}	S23
11. Figure S16. Plot of eq. [6] used to determine θ_2' for $^2J_{\text{C1',C3'}}$ values of 6.3 and 6.5 Hz in 8 ^{1',3'}	S24
12. Description of aqueous (1- μs) molecular dynamics simulations	S25
13. Discussion of equation [1] for J -coupling equation parameterization	S25
14. Representative Cartesian coordinates for 1 ^c , 6 ^c , 7 ^c , 8 ^c and 9 ^c	S26–29
15. Complete reference 28	S30
16. Supporting Information references	S30–31

1. Chemical Synthesis, Solution and Solid-State NMR Spectra, and X-ray Crystallography of **6**^{1,3}

1.1. *Chemical Synthesis.* Methyl β -D-[1,3-¹³C₂]Xylopyranoside **6**^{1,3} was prepared by Fischer glycosylation of D-[1,3-¹³C₂]xylose in anhydrous methanol,¹ and purified by chromatography on a column containing Dowex 1 x 8 (200–400 mesh) ion-exchange resin in the OH⁻ form.²

1.2. Solution and Solid-State NMR Spectra

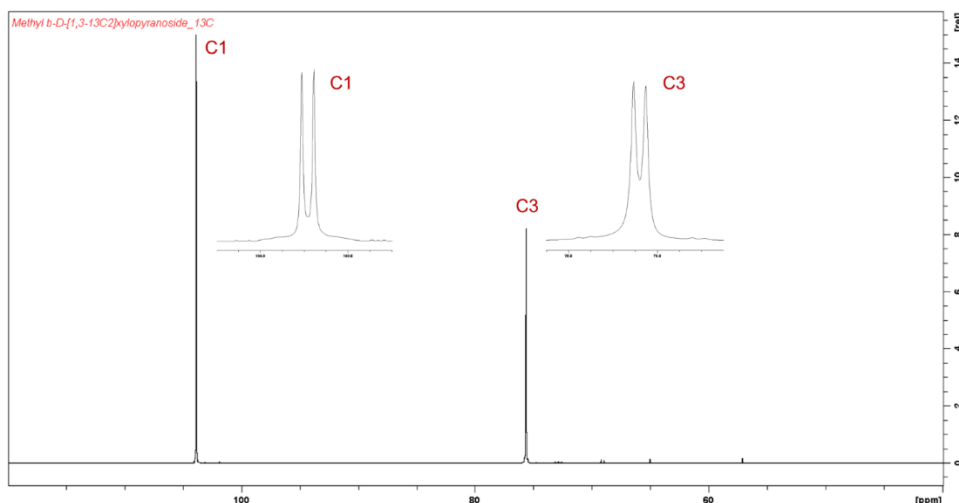


Figure S1. Partial ¹³C{¹H} NMR spectrum (150 MHz) of **6**^{1,3} showing the two signals arising from the ¹³C-labeled carbons (103.9 and 75.6 ppm) and their assignments. The weak signals between 55 and 75 ppm arise from the carbons at natural abundance. ²J_{C1,C3} (4.2 Hz) was measured from the splitting of the C1 and C3 signals (insets).

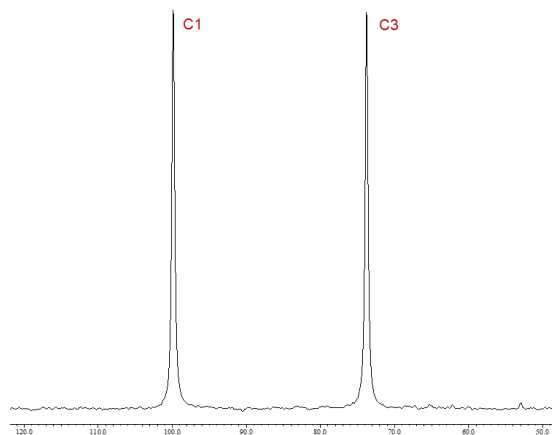


Figure S2. Partial cross-polarization magic-angle spinning (CP-MAS) 1D ¹³C NMR spectrum (75 MHz) of **6**^{1,3} showing signals arising only from the ¹³C-labeled carbons (99.9 and 73.8 ppm) and their assignments. The linewidths were 31.8 Hz (C1) and 31.5 Hz (C3).

1.3. *X-ray Crystallography.* Compound **6**^{1,3} was crystallized from a concentrated methanol solution at room temperature. The structure (nd1909) was re-determined at low temperature to obtain more accurate exocyclic torsion angles involving the hydroxyl hydrogens. The re-determined structure was essentially identical to that reported previously.³ The presence of ¹³C labeling in the compound did not alter the crystal structure in any appreciable fashion. Hydroxyl hydrogen atoms were located from a difference Fourier map and refined freely. The C1–C2–O2–H torsion angle θ_2 , measured using the atomic coordinates in Table S1, is $85.05^\circ \pm 3^\circ$.

Table S1. Atomic coordinates and equivalent isotropic displacement parameters (\AA^2) for **6**^{1,3} (nd1909). $U_{(\text{eq})}$ is defined as one third of the trace of the orthogonalized U_{ij} tensor.

	x	y	z	$U_{(\text{eq})}$
O(1)	0.6800(2)	0.6809(2)	-0.0219(2)	0.021(1)
O(2)	0.5126(2)	0.7817(2)	0.2321(2)	0.022(1)
O(3)	0.4729(2)	0.4696(2)	0.4452(2)	0.022(1)
O(4)	0.8084(2)	0.2176(2)	0.5792(2)	0.022(1)
O(5)	0.7870(2)	0.3996(2)	0.1322(2)	0.021(1)
C(1)	0.7362(3)	0.5937(3)	0.1526(3)	0.018(1)
C(2)	0.5690(3)	0.5918(3)	0.2109(3)	0.017(1)
C(3)	0.6332(3)	0.4889(3)	0.3993(3)	0.018(1)
C(4)	0.7179(3)	0.2924(3)	0.3936(3)	0.019(1)
C(5)	0.8661(3)	0.3060(3)	0.3112(3)	0.022(1)
C(6)	0.8370(3)	0.7151(4)	-0.0733(3)	0.030(1)
H(2O)	0.437(5)	0.817(6)	0.123(5)	0.053(11)
H(3O)	0.499(5)	0.408(6)	0.537(5)	0.041(9)
H(4O)	0.734(5)	0.137(5)	0.603(4)	0.034(8)
H(1)	0.84681	0.66311	0.24817	0.021
H(2)	0.45962	0.52165	0.11464	0.021
H(3)	0.73131	0.56898	0.49766	0.021
H(4)	0.61436	0.20321	0.31545	0.022
H(5A)	0.97737	0.37917	0.39755	0.027
H(5B)	0.90938	0.17573	0.29644	0.027
H(6A)	0.79645	0.80064	-0.18253	0.045
H(6B)	0.88016	0.59304	-0.10475	0.045
H(6C)	0.94125	0.77499	0.03227	0.045

2. Chemical Synthesis, Solution and Solid-State NMR Spectra, and X-ray Crystallography of **7**^{1,3}

2.1. *Chemical Synthesis.* Methyl β -D-[1,3-¹³C₂]Galactopyranoside **7**^{1,3} was prepared and purified by the same methods described for **6**^{1,3} starting from D-[1,3-¹³C₂]galactose.

2.2. Solution and Solid-State NMR Spectra

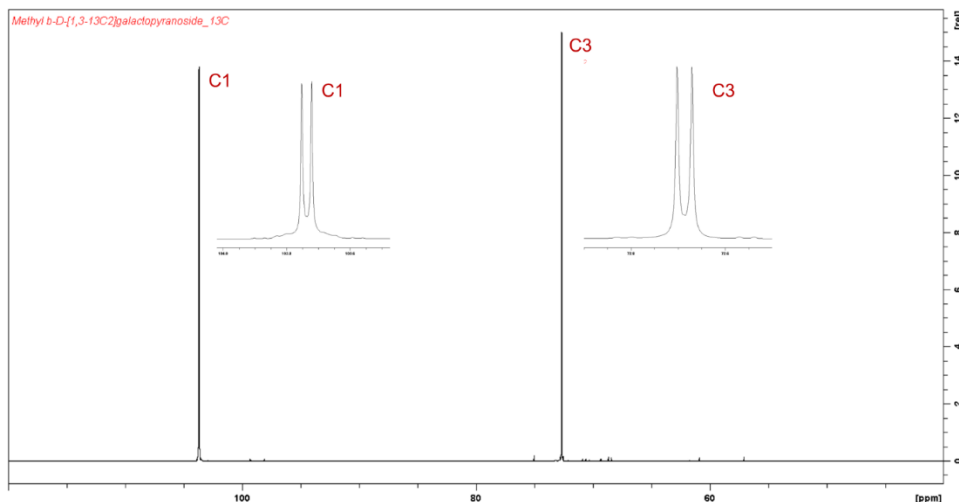


Figure S3. Partial ¹³C{¹H} NMR spectrum (150 MHz) of **7**^{1,3} showing the two signals arising from the ¹³C-labeled carbons (103.7 and 72.7 ppm) and their assignments. The weak signals between 55 and 75 ppm arise from the carbons at natural abundance. ²J_{C1,C3} (4.7 Hz) was measured from the splitting of the C1 and C3 signals (insets).

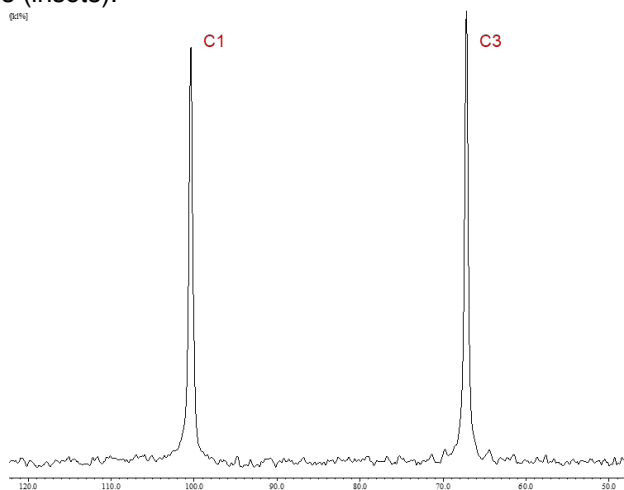


Figure S4. Partial cross-polarization magic-angle spinning (CP-MAS) 1D ¹³C NMR spectrum (75 MHz) of **7**^{1,3} showing signals arising only from the ¹³C-labeled carbons (100.4 and 67.2 ppm) and their assignments. The linewidths were 40.3 Hz (C1) and 38.6 Hz (C3).

2.3. *X-ray Crystallography.* Compound **7**^{1,3} was crystallized from a concentrated methanol solution at room temperature. The structure (nd1908) was re-determined at low temperature to obtain more accurate exocyclic torsion angles involving the hydroxyl hydrogens. The re-determined structure was essentially identical to those reported previously.^{4–6} The presence of ¹³C labeling in the compound did not alter the crystal structure in any appreciable fashion. Hydroxyl hydrogen atoms were located from a difference Fourier map and refined freely. The C1–C2–O2–H torsion angle θ_2 , measured using the atomic coordinates in Table S2, is $100.03^\circ \pm 3^\circ$.

Table S2. Atomic coordinates and equivalent isotropic displacement parameters (\AA^2) for **7**^{1,3} (nd1908). $U_{\text{(eq)}}$ is defined as one third of the trace of the orthogonalized U_{ij} tensor.

	x	y	z	U(eq)
O(1)	0.67504(17)	0.45820(15)	0.50976(9)	0.018(1)
O(2)	0.35148(17)	0.58029(16)	0.43194(11)	0.018(1)
O(3)	0.38329(17)	0.87684(16)	0.33006(10)	0.019(1)
O(4)	0.73307(16)	0.94338(15)	0.37282(9)	0.014(1)
O(5)	0.82179(16)	0.61422(14)	0.39792(9)	0.014(1)
O(6)	1.12123(17)	0.62137(15)	0.27105(10)	0.018(1)
C(1)	0.6611(2)	0.5367(2)	0.41629(12)	0.014(1)
C(2)	0.5148(2)	0.6571(2)	0.42359(13)	0.013(1)
C(3)	0.5108(2)	0.7563(2)	0.32575(13)	0.013(1)
C(4)	0.6885(2)	0.8236(2)	0.29992(12)	0.012(1)
C(5)	0.8220(2)	0.6906(2)	0.29915(13)	0.013(1)
C(6)	1.0032(2)	0.7496(2)	0.27813(14)	0.015(1)
C(7)	0.7729(3)	0.3153(2)	0.50162(16)	0.027(1)
H(2O)	0.321(3)	0.579(3)	0.488(2)	0.019(6)
H(3O)	0.365(5)	0.903(4)	0.393(3)	0.048(9)
H(4O)	0.788(3)	1.012(3)	0.3385(19)	0.022(6)
H(6O)	1.187(4)	0.617(3)	0.325(2)	0.039(8)
H(1)	0.63657	0.45977	0.36009	0.017
H(2)	0.53359	0.72683	0.48439	0.016
H(3)	0.47783	0.6843	0.26832	0.016
H(4)	0.68368	0.87197	0.23006	0.015
H(5)	0.78937	0.61211	0.24535	0.015
H(6A)	1.00426	0.80984	0.21315	0.019
H(6B)	1.0398	0.82116	0.334	0.019
H(7A)	0.77099	0.2599	0.56753	0.04
H(7B)	0.89281	0.34025	0.48316	0.04
H(7C)	0.72177	0.24802	0.44859	0.04

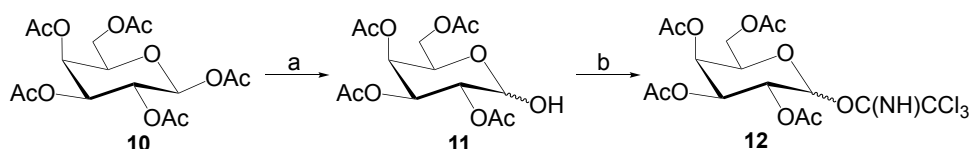
3. Chemical Synthesis, Solution and Solid-State NMR Spectra, and X-ray Crystallography of **8**^{1,3}

3.1. Chemical Synthesis

2,3,4,6-Tetra-*O*-acetyl- α -D-galactopyranosyl Trichloroacetimidate (12**).** Benzyl amine (1.46 mL, 13.83 mmol) was added to a solution of penta-*O*-acetyl- α/β -D-galactopyranose **10** (4.33 g, 11.10 mmol) in THF (50 mL) with stirring and the resulting mixture was stirred at rt for 3 h. The reaction mixture was then concentrated *in vacuo* at 45 °C to ~10 mL. The concentrated reaction mixture was diluted with ethyl acetate and washed by 0.1 *M* aqueous HCl, saturated aqueous NaHCO₃ solution, and

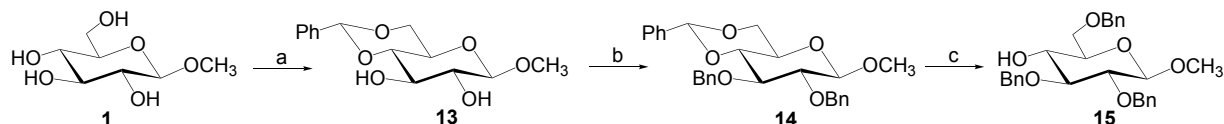
distilled water. The organic layer was isolated and dried at rt *in vacuo* for 2 h to afford 2,3,4,6-tetra-*O*-acetyl- α/β -

Synthesis of Donor **12**



D-galactopyranose **11** as a syrup. The syrup was dissolved in 50 mL anhydrous CH₂Cl₂, and CCl₃CN (5.56 mL, 55.45 mmol) and DBU (200 μ L, 1.34 mmol) were added to the mixture with stirring. The mixture was stirred at rt for 2 h. The reaction mixture was then concentrated *in vacuo* under 35 °C and applied to a 14 cm x 3.5 cm column of silica gel (hexane-ethyl acetate gradient elution) to afford 2,3,4,6-tetra-*O*-acetyl- α/β -D-galactopyranosyl trichloroacetimidate **12** in 53% yield (2.90 g, 5.88 mmol).

Synthesis of Acceptor **15**



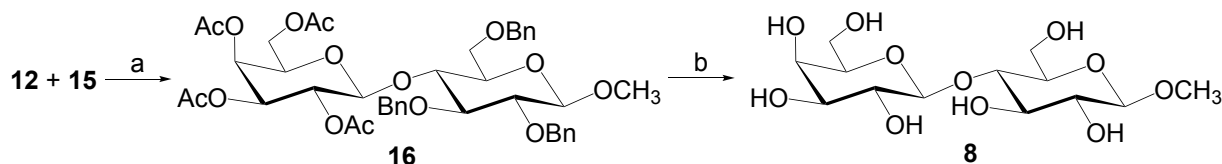
Methyl 4,6-*O*-Benzylidene- β -D-glucopyranoside (13**).** Benzaldehyde dimethyl acetal (1.85 mL, 12.36 mmol) and *p*-toluenesulfonic acid (39 mg, 0.21 mmol) were added to a solution of methyl β -D-glucopyranoside **1** (2.00 g, 10.30 mmol) in anhydrous DMF (20 mL) with stirring, and the resulting mixture was stirred at 60 °C for 2 h. The reaction was quenched with the addition of Et₃N (1 mL). The reaction mixture was concentrated *in vacuo* and dried to afford a solid. The solid was washed two times with a minimum volume of CH₃CN and dried *in vacuo* to give methyl 4,6-*O*-benzylidene- β -D-glucopyranoside **13** in 41% yield (1.19 g, 4.22 mmol). Compound **9** was used in the following step without further purification.

Methyl 2,3-Di-*O*-benzyl-4,6-*O*-benzylidene- β -D-glucopyranoside (14**).** NaH (60% w/w, 0.84 g, 21.08 mmol) and benzyl bromide (2.51 mL, 21.08 mmol) were added to a solution of methyl 4,6-*O*-benzylidene- β -D-glucopyranoside **13** (1.19 g, 4.22 mmol) in DMF (20 mL) with stirring, and the resulting mixture was stirred at rt overnight. The reaction was then quenched with the addition of methanol (20 mL) in 0 °C, and the reaction mixture was concentrated *in vacuo* at 50 °C. The concentrated reaction mixture was extracted by ethyl acetate/water two times. The organic layers were collected and concentrated at 40 °C *in vacuo*, and the residue was dried *in vacuo* for 2 h to

afford methyl 2,3-di-*O*-benzyl-4,6-*O*-benzylidene- β -D-glucopyranoside **14** in quantitative yield (1.95 g, 4.22 mmol).

Methyl 2,3,6-Tri-*O*-benzyl- β -D-glucopyranoside (15**).** Triethylsilane (6.73 mL, 42.16 mmol) and BF_3OEt_2 (1.04 mL, 8.43 mmol) were added to a solution of methyl 2,3-di-*O*-benzyl-4,6-*O*-benzylidene- β -D-glucopyranoside **14** (1.95 g, 4.22 mmol) with stirring, and the reaction mixture was stirred at 0 °C for 3 h. The reaction was then quenched with the addition of Et_3N (2 mL). The reaction mixture was concentrated *in vacuo* at 40 °C and the sample was purified on a 12 cm x 2.5 cm chromatographic column of silica gel (hexane-ethyl acetate gradient elution) to afford methyl 2,3,6-tri-*O*-benzyl- β -D-glucopyranoside **15** in 62% yield (1.22 g, 2.63 mmol).

Synthesis of Disaccharide **8** Using Donor **12** and Acceptor **15**



Reagents and conditions: (a) TMSOTf, 4 Å MS, DCM, 67%; (b) MeONa, MeOH, quant; H_2 , Pd/C, MeOH, quant.

Methyl 2,3,4,6-Tetra-*O*-acetyl- β -D-galactopyranosyl-(1→4)-2,3,6-tri-*O*-benzyl- β -D-glucopyranoside (12**).** A mixture of 2,3,4,6-tetra-*O*-acetyl- α/β -D-galactopyranosyl trichloroacetimidate **12** (383 mg, 0.51 mmol), methyl 2,3,6-tri-*O*-benzyl- β -D-glucopyranoside **15** (160 mg, 0.34 mmol), and freshly activated 4 Å molecular sieves in anhydrous DCM (10 mL) was stirred under nitrogen at 0 °C. TMSOTf (40 μL) was added, and the resulting mixture was stirred at 0 °C for 2 h. The reaction was then quenched with the addition of Et_3N (100 μL). The mixture was filtered, the solids were washed with DCM, and the filtrates were collected and concentrated at 40 °C *in vacuo*. The resulting mixture was purified by column chromatography (12 cm x 2.5 cm) on silica gel (hexane-ethyl acetate gradient elution) to afford methyl 2,3,4,6-tetra-*O*-acetyl- β -D-galactopyranosyl-(1→4)-2,3,6-tri-*O*-benzyl- β -D-glucopyranoside **16** in 67% yield (183 mg, 0.23 mmol).

Methyl β -D-Galactopyranosyl-(1→4)- β -D-glucopyranoside (8**).** Sodium methoxide (25% w/w in MeOH; 0.6 mL) was added to a solution of methyl 2,3,4,6-tetra-*O*-acetyl- β -D-galactopyranosyl-(1→4)-2,3,6-tri-*O*-benzyl- β -D-glucopyranoside **16** (183 mg, 0.23 mmol) in methanol (15 mL) with stirring, and the resulting mixture was stirred at rt for 2 h. The reaction mixture was then neutralized with the addition of Dowex 50 x 8 (200–400 mesh) resin in the H^+ form. The mixture was filtered, and the filtrate was concentrated *in vacuo* at 40 °C, and the residue dried *in vacuo* for 2 h. The dried residue was dissolved in methanol (20 mL), and a catalytic amount of Pd/C was added. The resulting mixture was stirred at rt under an H_2 atmosphere overnight. The mixture was then filtered, and the filtrate was collected, concentrated at 40 °C *in vacuo*, and the residue was dried *in vacuo*. The resulting solid was dissolved in a minimal volume of distilled water and the solution was applied to a chromatographic column (110 cm x 8 cm) containing Biogel P2 (45–90 μm). Column elution with distilled water afforded methyl β -D-galactopyranosyl-(1→4)- β -D-glucopyranoside **8** in quantitative yield (82 mg, 0.23 mmol).

Methyl β -D-Galactopyranosyl-(1→4)- β -D-[1,3- $^{13}\text{C}_2$]glucopyranoside (**8**^{1,3}) was prepared using D-[1,3- $^{13}\text{C}_2$]glucose (**1**^{1,3}) in the synthesis of acceptor **15**^{1,3}.

3.2. Solution and Solid-State NMR Spectra

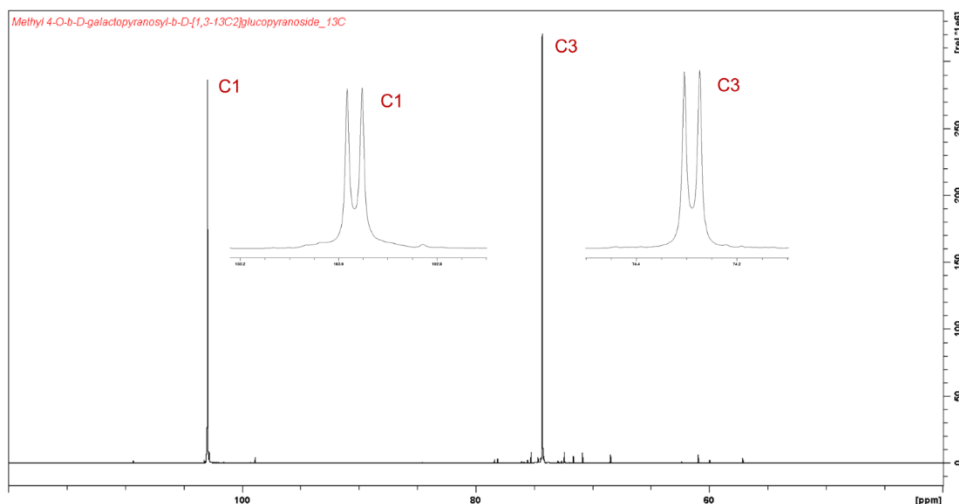


Figure S5. Partial $^{13}\text{C}\{^1\text{H}\}$ NMR spectrum (150 MHz) of **8**^{1,3} showing the two signals arising from the ^{13}C -labeled carbons (103.0 and 74.3 ppm) and their assignments. The weak signals between 55 and 80 ppm arise from the carbons at natural abundance. $^2J_{\text{C1,C3}}$ (4.6 Hz) was measured from the splitting of the C1 and C3 signals (insets).

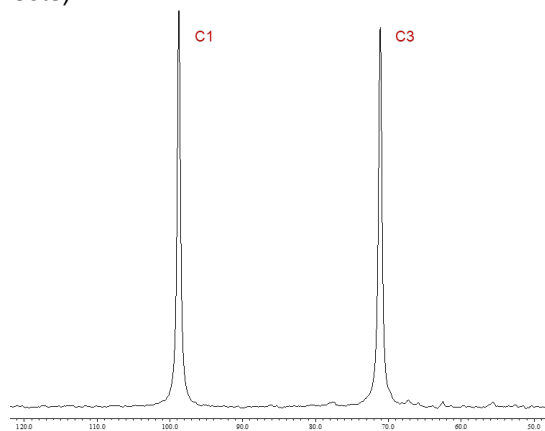


Figure S6. Partial cross-polarization magic-angle spinning (CP-MAS) 1D ^{13}C NMR spectrum (75 MHz) of **8**^{1,3} showing signals arising only from the ^{13}C -labeled carbons (98.8 and 71.1 ppm) and their assignments. The linewidths were 36.0 Hz (C1) and 40.1 Hz (C3).

3.3. X-ray Crystallography. Disaccharide **8**^{1,3} was crystallized from a concentrated methanol solution at room temperature. The structure (nd1917) was re-determined at low temperature to obtain more accurate exocyclic torsion angles involving the hydroxyl hydrogens. The re-determined structure was essentially identical to that reported previously.⁷ The presence of ^{13}C labeling in the compound did not alter the crystal structure in any appreciable fashion. Hydroxyl hydrogen atoms were located from a difference Fourier map and refined freely. The C1–C2–O2–H torsion angle θ_2 , measured using the atomic coordinates in Table S3, is $234.1^\circ \pm 3^\circ$.

Table S3. Atomic coordinates and equivalent isotropic displacement parameters (\AA^2) for **8**^{1,3} (nd1917). U_{eq} is defined as one third of the trace of the orthogonalized U_{ij} tensor.

	x	y	z	U(eq)
O(1)	0.2540(8)	0.68903(13)	-0.1543(4)	0.030(1)
O(2)	0.0762(8)	0.58520(13)	-0.2714(4)	0.029(1)
O(3)	0.4110(8)	0.50744(12)	-0.0206(4)	0.029(1)
O(5)	0.3748(7)	0.66209(12)	0.1371(4)	0.026(1)
O(6)	0.7798(7)	0.65485(13)	0.4713(4)	0.027(1)
C(1)	0.1915(10)	0.65108(18)	-0.0378(6)	0.026(1)
C(2)	0.2731(10)	0.59689(17)	-0.0987(6)	0.025(1)
C(3)	0.2666(10)	0.55234(16)	0.0345(5)	0.024(1)
C(4)	0.4220(10)	0.56962(16)	0.2286(5)	0.023(1)
C(5)	0.3145(9)	0.62519(17)	0.2660(5)	0.023(1)
C(6)	0.4645(10)	0.64642(17)	0.4508(6)	0.025(1)
C(7)	0.1172(14)	0.73975(19)	-0.1456(7)	0.039(1)
O(1')	0.3453(7)	0.53526(12)	0.3581(4)	0.025(1)
O(2')	0.6843(7)	0.50156(13)	0.7063(4)	0.027(1)
O(3')	0.6905(7)	0.38806(13)	0.7715(4)	0.027(1)
O(4')	0.2039(7)	0.35959(13)	0.4675(4)	0.026(1)
O(5')	0.3213(7)	0.44878(12)	0.2620(4)	0.023(1)
O(6')	0.2622(7)	0.39441(13)	-0.0485(4)	0.027(1)
C(1')	0.4944(10)	0.48609(16)	0.3884(6)	0.023(1)
C(2')	0.5092(9)	0.46538(16)	0.5755(5)	0.023(1)
C(3')	0.6584(9)	0.41015(17)	0.5978(5)	0.023(1)
C(4')	0.4969(9)	0.37131(16)	0.4509(6)	0.024(1)
C(5')	0.4741(9)	0.39800(16)	0.2706(5)	0.023(1)
C(6')	0.2899(10)	0.36539(18)	0.1138(5)	0.027(1)
O(1S)	0.8673(10)	0.76026(15)	0.4229(5)	0.042(1)
C(1S)	0.9081(13)	0.7617(2)	0.2474(7)	0.038(1)
H(2)	-0.003(19)	0.556(4)	-0.267(12)	0.06(2)
H(3)	0.351(12)	0.475(2)	0.035(7)	0.022(12)
H(6)	0.88(2)	0.631(4)	0.577(14)	0.08(3)
H(1)	-0.02616	0.65217	-0.04053	0.031
H(2A)	0.4825	0.59927	-0.11143	0.03
H(3A)	0.05261	0.54283	0.02534	0.028
H(4)	0.64506	0.56996	0.24809	0.028
H(5)	0.09246	0.62381	0.25015	0.028
H(6A)	0.36921	0.68066	0.4697	0.03
H(6B)	0.4377	0.62053	0.542	0.03

H(7A)	0.14448	0.76273	-0.24252	0.058
H(7B)	0.21109	0.75664	-0.02994	0.058
H(7C)	-0.09806	0.73477	-0.1585	0.058
H(2')	0.631(18)	0.499(3)	0.807(11)	0.05(2)
H(3')	0.551(14)	0.390(2)	0.810(8)	0.025(13)
H(4')	0.193(17)	0.327(3)	0.500(10)	0.046(19)
H(6')	0.077(16)	0.396(3)	-0.118(9)	0.037(16)
H(1')	0.70132	0.48955	0.37254	0.028
H(2'A)	0.30148	0.46247	0.5906	0.027
H(3'A)	0.86596	0.41519	0.58426	0.028
H(4'A)	0.6155	0.33741	0.46012	0.028
H(5')	0.68048	0.4039	0.2562	0.027
H(6'A)	0.38966	0.33056	0.10827	0.033
H(6'B)	0.08796	0.35827	0.12986	0.033
H(1S)	0.854(17)	0.727(3)	0.449(9)	0.046(18)
H(1SA)	1.11654	0.75238	0.25304	0.056
H(1SB)	0.86385	0.79781	0.19749	0.056
H(1SC)	0.77186	0.73592	0.17081	0.056

4. Chemical Synthesis, Solution and Solid-State NMR Spectra, and X-ray Crystallography of **8**^{1',3'}

4.1. *Chemical Synthesis.* Methyl β -D-[1,3-¹³C₂]galactopyranosyl-(1 \rightarrow 4)- β -D-glucopyranoside (**8**^{1',3'}) was prepared as described for methyl β -D-galactopyranosyl-(1 \rightarrow 4)- β -D-[1,3-¹³C₂]glucopyranoside (**8**^{1,3}) using D-[1,3-¹³C₂]galactose in the synthesis of donor **12**^{1,3} (see Section 3.1)

4.2. Solution and Solid-State NMR Spectra

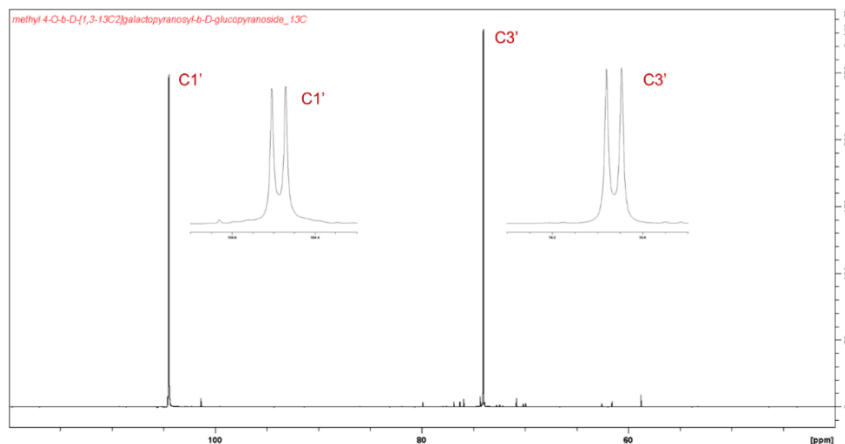


Figure S7. Partial ¹³C{¹H} NMR spectrum (150 MHz) of **8**^{1',3'} showing the two signals arising from the ¹³C-labeled carbons (104.5 and 74.1 ppm) and their assignments. The weak signals between 55 and 80 ppm arise from the carbons at natural abundance. ²J_{C1',C3'} (5.1 Hz) was measured from the splitting of the C1 and C3 signals (insets).

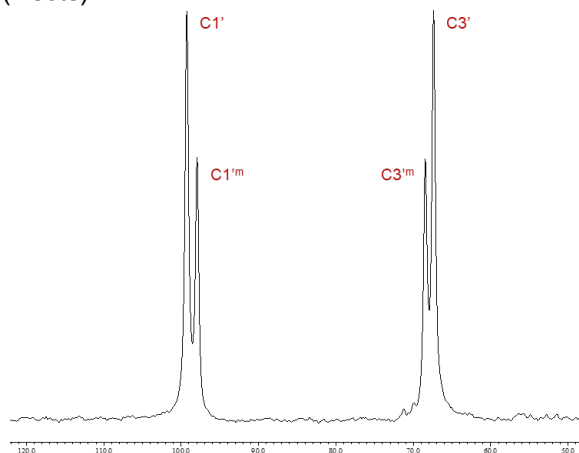


Figure S8. Partial cross-polarization magic-angle spinning (CP-MAS) 1D ¹³C NMR spectrum (75 MHz) of **8**^{1',3'} showing signals arising only from the ¹³C-labeled carbons. Two crystalline forms are observed, with the major form contributing signals C1' (99.3 ppm) and C3' (67.4 ppm) and the minor form contributing signals C1'^m (97.9 ppm) and C3'^m (68.5 ppm). The linewidths were as follows: 41.0 Hz (C1'); 38.3 Hz (C1'^m); 38.3 Hz (C3'); 39.8 Hz (C3'^m).

4.3. *X-ray Crystallography.* Compound **8**^{1',3'} was crystallized from a concentrated methanol solution at room temperature. The structure (nd1916) was re-determined at low temperature to obtain more accurate exocyclic torsion angles involving the hydroxyl hydrogens. The re-determined structure was essentially identical to that reported previously.⁷ The presence of ¹³C labeling in the compound did not alter the crystal structure in any appreciable fashion. Hydroxyl hydrogen atoms were located from a difference Fourier map and refined freely. The C1'–C2'–O2'–H torsion angle θ_2' , measured using the atomic coordinates in Table S4, is $146.65^\circ \pm 3^\circ$.

Table S4. Atomic coordinates and equivalent isotropic displacement parameters (\AA^2) for **8**^{1',3'} (nd1916). $U_{\text{(eq)}}$ is defined as one third of the trace of the orthogonalized U_{ij} tensor.

	x	y	z	U(eq)
O(1)	0.7461(4)	0.68886(7)	1.1545(2)	0.021(1)
O(2)	0.9233(4)	0.58524(7)	1.2708(2)	0.021(1)
O(3)	0.5880(4)	0.50757(6)	1.0203(2)	0.020(1)
O(5)	0.6262(4)	0.66209(6)	0.8627(2)	0.017(1)
O(6)	0.2209(4)	0.65495(7)	0.5288(2)	0.019(1)
C(1)	0.8089(5)	0.65110(9)	1.0380(3)	0.017(1)
C(2)	0.7276(5)	0.59660(9)	1.0991(3)	0.016(1)
C(3)	0.7332(5)	0.55226(9)	0.9645(3)	0.016(1)
C(4)	0.5787(5)	0.56956(9)	0.7714(3)	0.015(1)
C(5)	0.6866(5)	0.62527(9)	0.7350(3)	0.016(1)
C(6)	0.5345(5)	0.64640(9)	0.5486(3)	0.017(1)
C(7)	0.8819(7)	0.73976(10)	1.1453(4)	0.029(1)
O(1')	0.6557(4)	0.53505(6)	0.6416(2)	0.016(1)
O(2')	0.3159(4)	0.50141(7)	0.2934(2)	0.019(1)
O(3')	0.3095(4)	0.38800(7)	0.2291(2)	0.019(1)
O(4')	0.7967(3)	0.35959(7)	0.5323(2)	0.018(1)
O(5')	0.6781(4)	0.44859(6)	0.7377(2)	0.016(1)
O(6')	0.7378(4)	0.39445(7)	1.0486(2)	0.019(1)
C(1')	0.5062(5)	0.48613(9)	0.6119(3)	0.015(1)
C(2')	0.4901(5)	0.46561(8)	0.4238(3)	0.015(1)
C(3')	0.3420(5)	0.41012(9)	0.4022(3)	0.015(1)
C(4')	0.5043(5)	0.37133(8)	0.5495(3)	0.015(1)
C(5')	0.5269(5)	0.39804(9)	0.7295(3)	0.015(1)
C(6')	0.7096(5)	0.36560(9)	0.8860(3)	0.018(1)
O(1S)	0.8676(5)	0.26026(8)	0.4225(3)	0.033(1)
C(1S)	0.9090(7)	0.26163(12)	0.2478(4)	0.029(1)
H(2)	1.012(9)	0.5601(18)	1.276(6)	0.036(11)
H(3)	0.64566	0.47912	0.98213	0.03
H(6)	0.125(9)	0.6357(17)	0.439(6)	0.041(11)

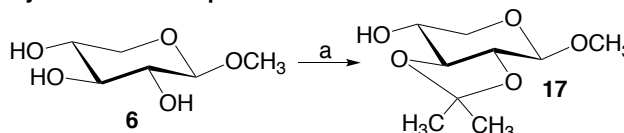
H(1)	1.02665	0.65226	1.04104	0.021
H(2A)	0.51815	0.59894	1.11182	0.019
H(3A)	0.94699	0.54258	0.97368	0.019
H(4)	0.35559	0.56991	0.75181	0.018
H(5)	0.90863	0.62394	0.75068	0.019
H(6A)	0.62994	0.68054	0.52886	0.021
H(6B)	0.56037	0.62031	0.45785	0.021
H(7A)	0.78722	0.75656	1.02963	0.044
H(7B)	1.09725	0.73492	1.15785	0.044
H(7C)	0.85464	0.76275	1.24205	0.044
H(2')	0.389(9)	0.5018(15)	0.200(5)	0.034(9)
H(3')	0.47543	0.38923	0.20424	0.028
H(4')	0.8041	0.32737	0.50247	0.026
H(6')	0.91978	0.39579	1.10664	0.029
H(1')	0.29939	0.48978	0.62793	0.018
H(2'A)	0.69777	0.46275	0.40859	0.017
H(3'A)	0.13447	0.41508	0.4158	0.018
H(4'A)	0.38573	0.33741	0.54049	0.018
H(5')	0.32033	0.40394	0.74353	0.018
H(6'A)	0.60942	0.33079	0.89127	0.022
H(6'B)	0.91163	0.35839	0.87015	0.022
H(1S)	0.855(9)	0.2285(19)	0.451(5)	0.038(10)
H(1SA)	0.77057	0.23625	0.1707	0.044
H(1SB)	1.11672	0.2517	0.25352	0.044
H(1SC)	0.86825	0.29787	0.19853	0.044

5. Chemical Synthesis, Solution and Solid-State NMR Spectra, and X-ray Crystallography of **9**^{1,3}

5.1. Chemical Synthesis

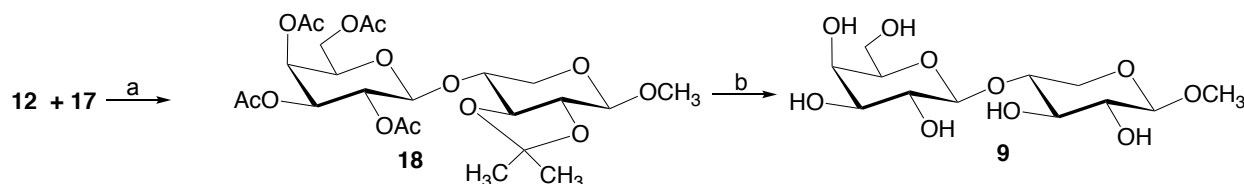
Methyl 2,3-*O*-Isopropylidene- β -D-xylopyranoside (17**).** Acetyl chloride (20 μ L) and methanol (100 μ L) were added to a solution methyl β -D-xylopyranoside **6** (0.30 g, 1.83 mmol) in anhydrous DMF (10 mL) under nitrogen. The resulting mixture was stirred at 0 $^{\circ}$ C for 15 min, 2-methoxypropene (0.70 mL, 7.31 mmol) was added dropwise over 10 min at 0 $^{\circ}$ C, and the reaction mixture was stirred at 0 $^{\circ}$ C for 2 h. The reaction mixture was then diluted with DCM (25 mL), and methanol (300 μ L) was added to transform the by-products back to the products. The mixture was stirred for 3 min, and pyridine (200 μ L) was added to quench the reaction. The mixture was extracted two times with DCM/water, and the organic layers was combined and dried *in vacuo* at 40 $^{\circ}$ C to give methyl 2,3-*O*-isopropylidene- β -D-xylopyranoside **17** in 75% yield as a solid (0.28 g, 1.37 mmol).

Synthesis of Acceptor **17**



Reagents and conditions: (a) 2-methoxypropene, AcCl/MeOH, DMF, 75%.

Synthesis of Disaccharide **9** Using Donor **12** and Acceptor **17**



Reagents and conditions: (a) TMSOTf, 4 \AA MS, DCM, 37%; (b) AcCl, MeOH; MeONa, MeOH, quant.

Methyl 2,3,4,6-Tetra-*O*-acetyl- β -D-galactopyranosyl-(1 \rightarrow 4)-2,3-*O*-Isopropylidene- β -D-xylopyranoside (18**).** A mixture of 2,3,4,6-tetra-*O*-acetyl- α / β -D-galactopyranosyl trichloroacetimidate **12** (350 mg, 0.71 mmol), methyl 2,3-*O*-isopropylidene- β -D-xylopyranoside **17** (130 mg, 0.61 mmol), and freshly activated 4 \AA molecular sieves in anhydrous DCM (10 mL) was stirred under nitrogen at 0 $^{\circ}$ C. TMSOTf (20 μ L) was added, and the resulting mixture was stirred at 0 $^{\circ}$ C for 2 h. Et₃N (100 μ L) was then added to quench the reaction. The mixture was filtered, the filter pad was washed with DCM, and the filtrates were collected and concentrated at 40 $^{\circ}$ C *in vacuo*. The crude product was purified on a 12 cm x 2.5 cm column of silica gel (hexane-ethyl acetate gradient elution) to give methyl 2,3,4,6-tetra-*O*-acetyl- β -D-galactopyranosyl-(1 \rightarrow 4)-2,3-*O*-isopropylidene- β -D-xylopyranoside **18** in 37% yield (120 mg, 0.22 mmol).

Methyl β -D-Galactopyranosyl-(1 \rightarrow 4)- β -D-xylopyranoside (9**).** Acetyl chloride (10 μ L) was added to a solution of methyl 2,3,4,6-tetra-*O*-acetyl- β -D-galactopyranosyl-(1 \rightarrow 4)-2,3-*O*-isopropylidene- β -D-xylopyranoside **18** (120 mg, 0.22 mmol) in methanol (10 mL) at 0 $^{\circ}$ C, and the resulting mixture was stirred for 2 h. Pyridine (100 μ L) was added to quench the reaction. Sodium methoxide solution (25% w/w in methanol, 0.6 mL) was added to the solution with stirring, and the resulting mixture was stirred at rt for 2 h. The reaction mixture was neutralized with the addition of Dowex 50 x 8 (200-400 mesh) resin in the H⁺ form, the resin was removed by filtration, the filtrate was concentrated at 40 $^{\circ}$ C *in vacuo*, and the residue was dried at rt *in vacuo*. The resulting solid was

dissolved in a minimal volume of distilled water and the solution was applied to a chromatographic column (110 cm x 3 cm) containing Biogel P2 (45–90 μm). Elution of the column with distilled water afforded methyl 4-*O*- β -D-galactopyranosyl- β -D-xylopyranoside **9** in quantitative yield (73 mg, 0.22 mmol).

Methyl β -D-galactopyranosyl-(1 \rightarrow 4)- β -D-[1,3- $^{13}\text{C}_2$]xylopyranoside (**9**^{1,3}) was prepared using D-[1,3- $^{13}\text{C}_2$]xylose (**2**^{1,3}) in the preparation of acceptor **17**^{1,3}.

5.2. Solution and Solid-State NMR Spectra

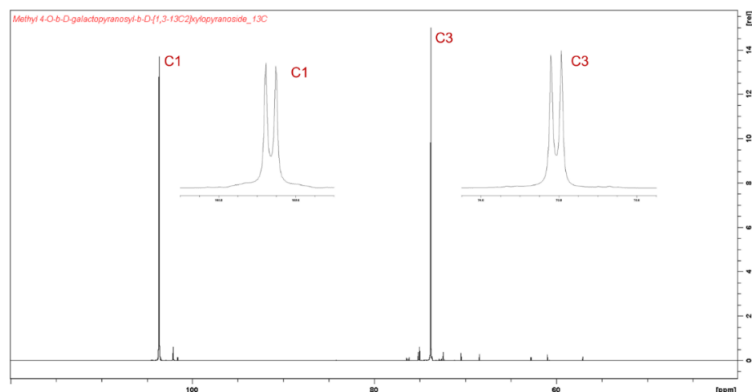


Figure S9. Partial $^{13}\text{C}\{^1\text{H}\}$ NMR spectrum (150 MHz) of **9**^{1,3} showing the two signals arising from the ^{13}C -labeled carbons (103.7 and 73.8 ppm) and their assignments. The compound may contain minor impurities. The weak signals between 55 and 80 ppm arise from the carbons at natural abundance. $^2J_{\text{C}1',\text{C}3'}$ (4.0 Hz) was measured from the splitting of the C1 and C3 signals (insets).

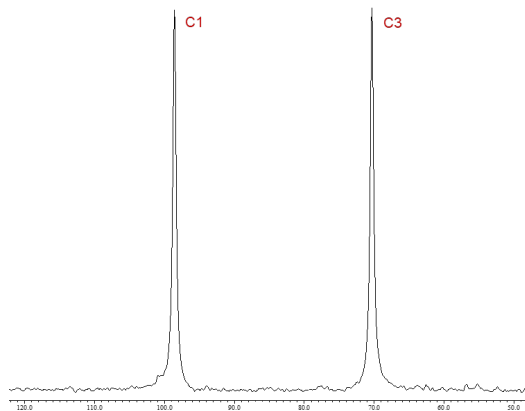


Figure S10. Partial cross-polarization magic-angle spinning (CP-MAS) 1D ^{13}C NMR spectrum (75 MHz) of **9**^{1,3} showing signals arising only from the ^{13}C -labeled carbons (98.6 and 70.3 ppm) and their assignments. The linewidths were 45.7 Hz (C1) and 44.0 Hz (C3).

5.3. X-ray Crystallography. Compound **9**^{1,3} was crystallized from a concentrated aqueous solution at room temperature.⁸ Its crystal structure was reported previously as CSD XAQL0S. The C1–C2–O2–H torsion angle θ_2 measured in this structure is $164.19^\circ \pm 3^\circ$.

6. Chemical Synthesis, Solution and Solid-State NMR Spectra, and X-ray Crystallography of **9**^{1',3'}

6.1. *Chemical Synthesis.* Methyl β -D-[1,3-¹³C₂]galactopyranosyl-(1 \rightarrow 4)- β -D-xylopyranoside (**9**^{1',3'}) was prepared as described for **9**^{1,3} (Section 5.1) using D-[1,3-¹³C₂]galactose in the synthesis of donor **12**^{1,3} (see Section 3.1).

6.2. Solution and Solid-State NMR Spectra

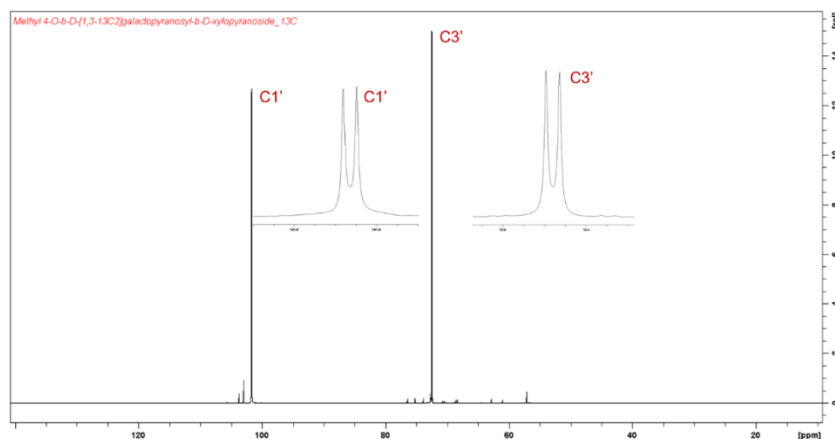


Figure S11. Partial ¹³C{¹H} NMR spectrum (150 MHz) of **9**^{1',3'} showing the two signals arising from the ¹³C-labeled carbons (101.7 and 72.5 ppm) and their assignments. The compound may contain minor impurities. The weak signals between 55 and 80 ppm arise from the carbons at natural abundance. ²J_{C1',C3'} (4.9 Hz) was measured from the splitting of the C1 and C3 signals (insets).

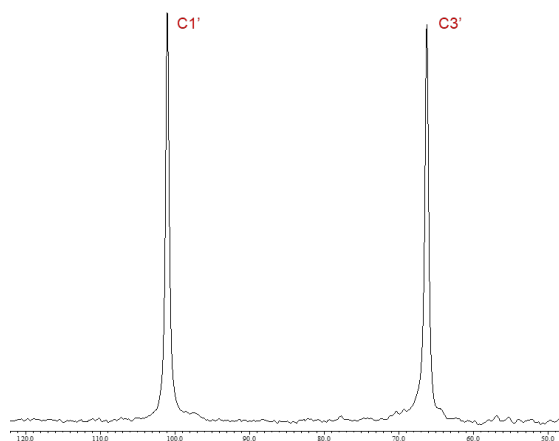


Figure S12. Partial cross-polarization magic-angle spinning (CP-MAS) 1D ¹³C NMR spectrum (75 MHz) of **9**^{1',3'} showing signals arising only from the ¹³C-labeled carbons (101.0 and 66.2 ppm) and their assignments. The linewidths were 39.5 Hz (C1) and 42.2 Hz (C3).

6.3. *X-ray Crystallography.* Disaccharide **9**^{1,3'} crystallizes from a concentrated aqueous solution at room temperature,⁸ and its crystal structure was reported previously as CSD XAQL0S. The C1'–C2'–O2'–H torsion angle θ_2' measured in this structure is $113.02^\circ \pm 3^\circ$.

7. X-ray Crystallography of **1**^{1,3}



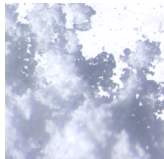
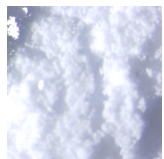
Compound **1**^{1,3} was prepared as described previously and crystallized from a concentrated aqueous solution at room temperature.⁹ The crystal structure of **1**^{1,3} was reported previously as CSD MBDGPH11. The C1–C2–O2–H torsion angle θ_2 measured in this structure is $91.5^\circ \pm 3^\circ$.

8. Effect of Solid-State NMR Sample Preparation on the Crystal Structure of **8**

Crystalline samples of **8**^{1,3} and **8**^{1',3'} that are grown in anhydrous methanol are homogenous in appearance. This appearance changes form during the removal of solvent (e.g. air-drying) or during operations involved in sample preparation for ssNMR measurements (e.g. air-drying, grinding and/or vacuum drying) (Table S5), resulting in a CP-MAS 1D ¹³C NMR spectrum of **8**^{1',3'} (but not of **8**^{1,3}) containing pairs of signals arising from the ¹³C-labeled carbons (Figure S8).

To evaluate the effect of sample preparation on the crystal structure of **8**, unlabeled **8** (170 mg) was crystallized from a solution of anhydrous methanol. The crystals were harvested and air-dried for ~96 h. A sample was withdrawn from the dried crystals (Sample 1), and three additional samples were withdrawn and treated separately to give Samples 2–4. (Table S5). Samples 1–4 were analyzed by X-ray powder diffraction (XRPD). Sample 1 was analyzed by single-crystal X-ray diffraction (SC-XRD).

Table S5. Four Samples of Crystalline **8** Obtained From Anhydrous MeOH and Subjected To Different Experimental Operations.

	Sample 1	Sample 2	Sample 3	Sample 4
Experimental Operation(s)	air-dry (~96 h)	air-dry (~96 h) grind	air-dry (~96 h) grind vacuum-dry (3 h)	air-dry (~96 h) grind twice vacuum-dry (17 h)
Physical Appearance	crystalline	powder	powder	powder
Sample Photo				

Solvomorphism was observed in Sample 1 by the low-temperature SC-XRD. The data indicate the presence of a water solvate form of crystalline **8** (denoted *blactob*), suggesting that hydrogen-bonded lattice MeOH is easily exchanged with hydrogen-bonded lattice H₂O extracted from the air during drying. The lattice water hydrogen atoms were located from a difference Fourier map and refined freely. The C1'–C2'–O2'–H torsion angle, θ_2' , measured using the atomic coordinates in Table S6, was found to be $154.48^\circ \pm 3^\circ$, which differs by 6.9° from that found the methanol-solvate crystal structure of **8**^{1',3'} (*nd1916*). The C1–C2–O2–H torsion angle, θ_2 , measured from the atomic coordinates in Table S6, is $234.64^\circ \pm 3^\circ$, which differs by 1.5° from that observed in the methanol solvate crystal structure of **8**^{1,3} (*nd1917*).

Since air-drying is required during ssNMR sample preparation, the methanol solvate form of crystalline **8** transforms, over longer periods of drying, to the water solvate form. The latter form is presumably more thermodynamically stable since the water participates in three hydrogen bonds to the saccharide in water solvate crystals of **8** compared to only two hydrogen bonds in methanol solvate crystals. The solid-state ¹³C NMR spectrum of **8**^{1',3'} shows the presence of the

water solvate form (minor peak, Figure S8), while it is unclear whether the sample used to obtain the solid-state ^{13}C NMR spectrum of **8**^{1,3} contains both crystalline forms since the chemical shifts of C1 and C3 are unaffected by solvate state (*i.e.*, these carbons are far from the sites of hydrogen bonding by either MeOH or H₂O (Figure S10). The C1–C2–O2–H torsion angle, θ_2 , in the *gluco* residue of **8** differs only slightly between the two crystalline forms (1.5°), which exerts virtually no effect on $^2J_{\text{C1,C3}}$ values.

Table S6. Atomic Coordinates and Equivalent Isotropic Displacement Parameters (\AA^2) for **8** (*blactob*).
[U_{eq} is defined as one-third of the trace of the orthogonalized U_{ij} tensor.]

	<i>x</i>	<i>y</i>	<i>z</i>	U_{eq}
O(1)	0.6945(4)	0.69849(7)	1.0028(2)	0.0275
O(1')	0.6438(3)	0.53275(6)	0.5092(2)	0.0212
O(1WA)	0.8828(5)	0.24834(8)	0.3890(3)	0.039
O(2)	0.8779(4)	0.59193(7)	1.1369(2)	0.0273
O(2')	0.2954(4)	0.50780(7)	0.1565(2)	0.0242
O(3)	0.5847(4)	0.50681(7)	0.8846(2)	0.0267
O(3')	0.2417(4)	0.39314(7)	0.0577(2)	0.0236
O(4')	0.7291(3)	0.35631(7)	0.3450(2)	0.0216
O(5)	0.5942(4)	0.66710(6)	0.7138(2)	0.022
O(5')	0.6327(3)	0.44224(6)	0.5922(2)	0.0205
O(6)	0.6390(4)	0.69673(7)	0.3572(2)	0.0326
O(6')	0.6741(4)	0.37160(8)	0.8886(2)	0.0309
C(1)	0.7704(5)	0.65761(9)	0.8945(3)	0.0224
C(1')	0.4761(5)	0.48398(9)	0.4699(3)	0.019
C(2)	0.6930(5)	0.60125(9)	0.9609(3)	0.0211
C(2')	0.4547(5)	0.46613(9)	0.2760(3)	0.0191
C(3)	0.7160(5)	0.55487(9)	0.8288(3)	0.0207
C(3')	0.2870(4)	0.41070(9)	0.2399(3)	0.0192
C(4)	0.5624(5)	0.57059(9)	0.6322(3)	0.0193
C(4')	0.4447(5)	0.36712(8)	0.3764(3)	0.0194
C(5)	0.6628(5)	0.62814(9)	0.5885(3)	0.0207
C(5')	0.4756(5)	0.38959(9)	0.5674(3)	0.0194
C(6)	0.5041(5)	0.64699(9)	0.3986(3)	0.0241
C(6')	0.6551(5)	0.35078(10)	0.7124(3)	0.0235
C(7)	0.8299(8)	0.75159(11)	0.9912(4)	0.0446
H(1)	0.989143	0.659576	0.901279	0.027
H(1')	0.270953	0.489821	0.486248	0.023
H(1WA)	0.754(11)	0.223(2)	0.368(6)	0.068

H(2)	0.480385	0.602811	0.967923	0.025
H(2')	0.660709	0.461727	0.25945	0.023
H(2O)	0.966(7)	0.5619(14)	1.139(4)	0.028
H(2O')	0.350(10)	0.5057(19)	0.072(6)	0.059
H(2WA)	1.061(10)	0.2309(17)	0.477(6)	0.056
H(3)	0.932872	0.547185	0.840473	0.025
H(3')	0.0842	0.416872	0.259449	0.023
H(3O)	0.620(7)	0.4790(15)	0.838(4)	0.03
H(3O')	0.383(10)	0.3858(17)	0.042(5)	0.047
H(4)	0.339661	0.570242	0.612083	0.023
H(4')	0.322924	0.332142	0.358138	0.023
H(4O')	0.763(6)	0.3252(13)	0.359(3)	0.013
H(5)	0.884393	0.627833	0.603711	0.025
H(5')	0.271254	0.394958	0.585586	0.023
H(6A)	0.517513	0.617523	0.310747	0.029
H(6'A)	0.859856	0.346429	0.697249	0.028
H(6B)	0.289315	0.65376	0.389118	0.029
H(6'B)	0.558665	0.313648	0.698278	0.028
H(6O)	0.669(8)	0.6930(14)	0.248(5)	0.041
H(6O')	0.873(8)	0.3795(14)	0.944(4)	0.039
H(A)	0.803777	0.761222	0.863564	0.067
H(B)	0.733905	0.780006	1.048469	0.067
H(C)	1.04454	0.749827	1.053489	0.067

X-ray powder diffraction (XRPD) spectra of Samples 1–4 are shown in Figure S13A. The four spectra are very similar, and differ significantly from that expected for the methanol solvate form (Figure S13B). These results show that air-drying alone is sufficient to exchange the lattice methanol for water, that is, grinding and/or vacuum drying (Samples 2–4) do not produce samples with XRPD spectra that differ much from that associated with Sample 1. Simulated XRPD spectra for the methanol solvate and water solvate are shown in Figure S13B, showing that spectra of the two forms differ significantly and that associated with the water hydrate more closely matches the XRPD spectra of Samples 1–4.

Facile methanol-water exchange in crystals of the methanol solvate of **8** was confirmed by obtaining a single-crystal X-ray structure of Sample 1 (Figure S14). This structure shows substitution of water at the original methanol site, resulting in small but discernible changes in the conformation of the disaccharide and changes in the hydrogen bonding between the solvent and disaccharide. The details of this new crystalline form of **8** will be reported elsewhere.

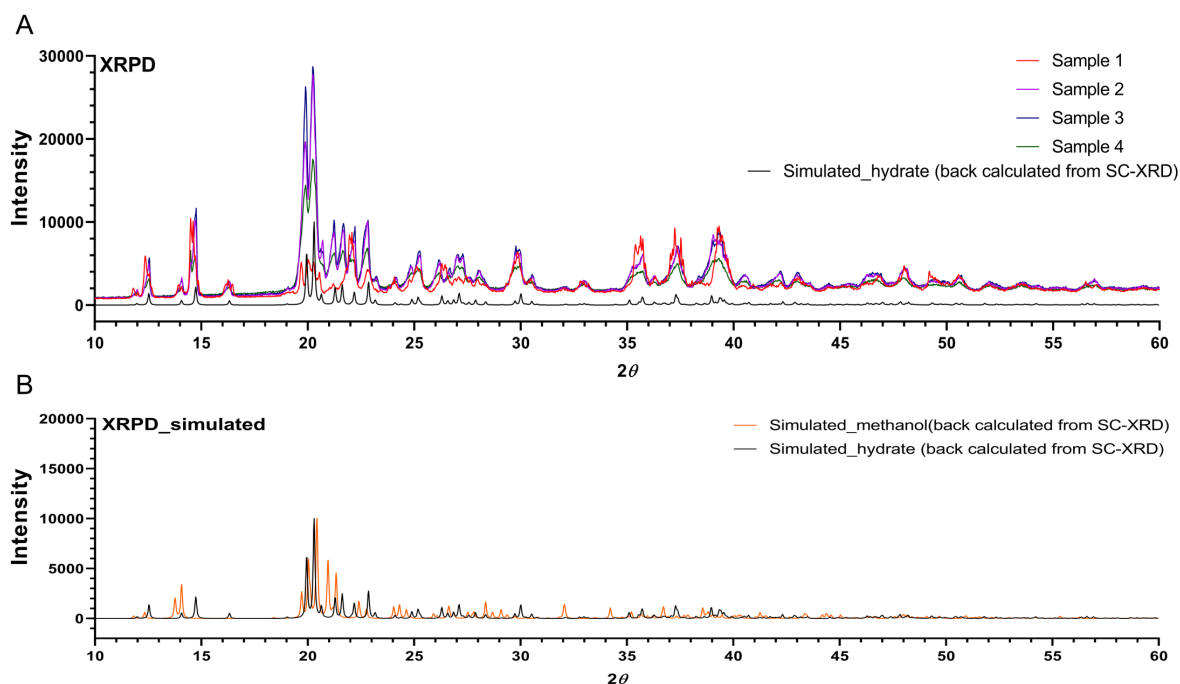


Figure S13. (Top Spectrum) Partial X-ray powder diffraction (XRPD) spectra of **8** obtained after different sample treatments (Table S5): Sample 1, red line; Sample 2, purple line; Sample 3, blue line; Sample 4, green line. The simulated XRPD spectrum was back-calculated based on the crystal structure of **8** in hydrate form (*blactob*). (Bottom Spectrum) Simulated XRPD spectra back-calculated from the SC-XRD structure of **8** in the methanol solvate form (*nd1916*, orange line) and the SC-XRD structure of **8** in the water solvate form (*blactob*, black line).

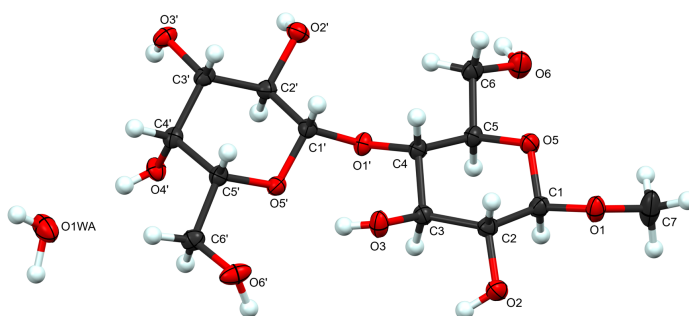


Figure S14. SC-XRD structure of methyl β -lactoside water solvate (*blactob*) showing a water molecule in the same binding pocket as that of methanol in the SC-XRD structure of methyl β -lactoside methanol solvate (*nd1916*). The crystals of the water solvate form were obtained by air-drying crystals of the methanol solvate form (Sample 1, Table S5). Cartesian coordinates of *blactob* are given in Table S6.

Table S7. Fitting Statistics from Solid-State ^{13}C NMR Measurements of $^2J_{\text{CCC}}$ Values in Crystalline **6**^{1,3}, **7**^{1,3}, **8**^{1,3}, **8**^{1',3'}, **9**^{1,3} and **9**^{1',3'}.

compound	$^2J_{\text{CCC}}$	J -coupling (Hz)	RMSE (Hz)	adjusted R^2
6 ^{1,3}	$^2J_{\text{C1,C3}}$	5.13	0.008	0.996
		5.14	0.007	0.997
		5.21	0.008	0.996
		5.22	0.028	0.950
		5.17	0.008	0.996
		5.19	0.008	0.995
7 ^{1,3}	$^2J_{\text{C1,C3}}$	4.74	0.010	0.990
		4.69	0.008	0.994
		4.73	0.010	0.991
		4.72	0.009	0.992
		4.80	0.007	0.996
		4.70	0.008	0.993
8 ^{1,3}	$^2J_{\text{C1,C3}}$	3.85	0.009	0.983
		3.84	0.006	0.992
		3.86	0.005	0.994
		3.75	0.005	0.993
		3.86	0.005	0.995
		3.82	0.009	0.982
8 ^{1',3'} (major form)	$^2J_{\text{C1'},\text{C3'}}$	6.30	0.008	0.998
		6.31	0.010	0.997
		6.34	0.011	0.996
		6.59	0.014	0.994
		6.69	0.015	0.994
		6.62	0.015	0.993
8 ^{1',3'} (minor form)	$^2J_{\text{C1'},\text{C3'}}$	6.14	0.012	0.994
		6.15	0.017	0.989
		6.22	0.017	0.989
		6.45	0.021	0.986
		6.45	0.022	0.985
		6.63	0.025	0.982
9 ^{1,3}	$^2J_{\text{C1,C3}}$	4.19	0.006	0.995
		4.15	0.005	0.996
		4.19	0.006	0.994
		4.15	0.004	0.997
		4.18	0.004	0.998
		4.19	0.005	0.996
9 ^{1',3'}	$^2J_{\text{C1'},\text{C3'}}$	6.52	0.011	0.996
		6.52	0.011	0.996
		6.53	0.012	0.996
		6.45	0.014	0.994
		6.53	0.009	0.998
		6.46	0.011	0.996

The top six measurements are shown, ranked by RMSE and adjusted R^2 .

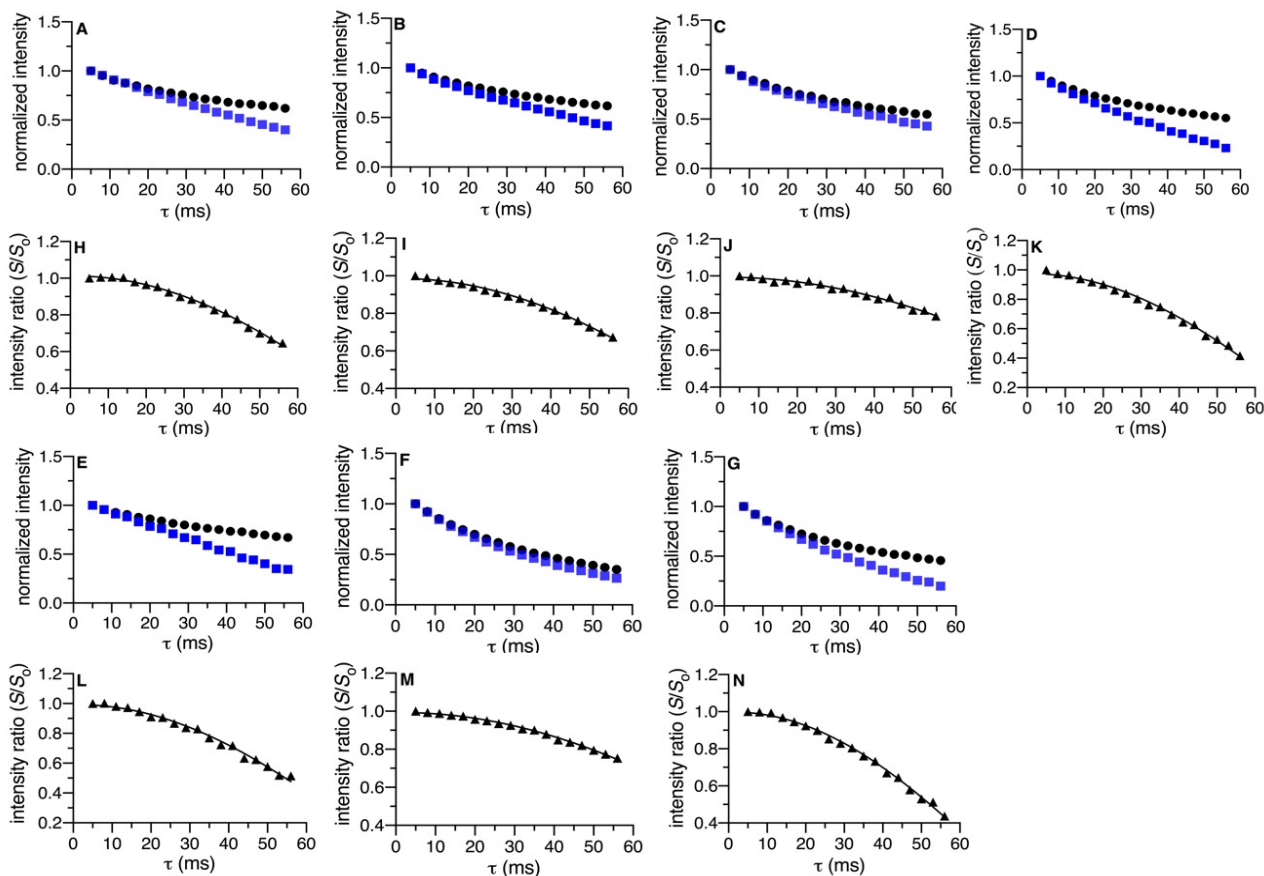


Figure S15. Plots of S/S_0 vs τ used to determine $^2J_{C1,C3}$ or $^2J_{C1',C3'}$ in $6^{1,3}$ (A and H), $7^{1,3}$ (B and I), $8^{1,3}$ (C and J), $8^{1',3'}$ (major form) (D and K), $8^{1',3'}$ (minor form) (E and L), $9^{1,3}$ (F and M) and $9^{1',3'}$ (G and N). (A–G) Normalized intensities of the J -modulated echo signals (S ; blue points) and the reference echo signals (S_0 ; black points) plotted against the total echo interval, τ . (H–N) Intensity ratios, (S/S_0), plotted against τ . The solid lines represent best fits to the equation given in references 10–12. All experiments were run in triplicate, and only one representative signal is shown for each compound.

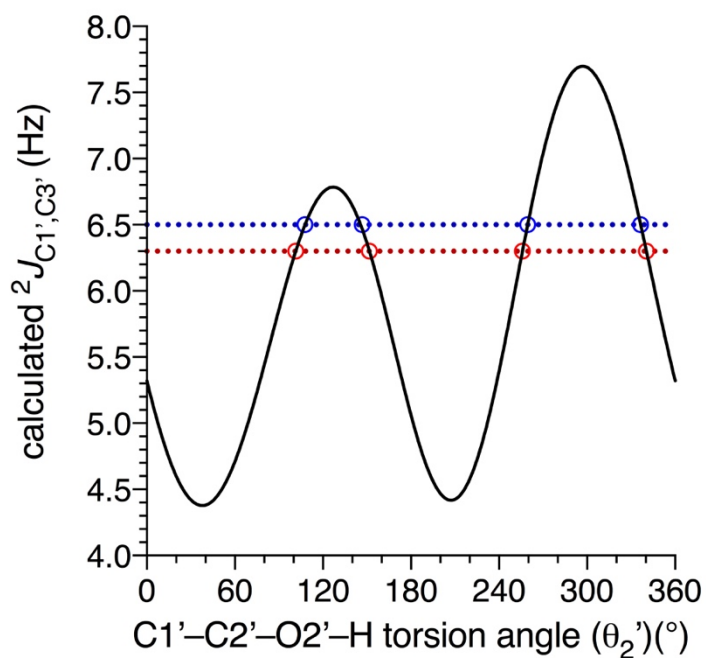


Figure S16. Plot of eq. [6] from which θ_2' in **8**^{1',3'} was determined from $^2J_{C1',C3'}$ values of 6.3 and 6.5 Hz. For 6.3 Hz (red dotted line), θ_2' can be 101°, 152°, 256° or 340°. For 6.5 Hz (blue dotted line), θ_2' can be 108°, 146°, 259° or 336°. See text for discussion.

Description of Aqueous (1- μ s) Molecular Dynamics Simulations

Initial structures of **1^c**, **7^c**, **8^c** and **9^c** were built using the Carbohydrate Builder module available at the GLYCAM website (<http://www.glycam.org>).¹³ The GLYCAM06¹⁴ (version j) force field was employed in all simulations. Structures **1^c**, **7^c**, **8^c** and **9^c** were solvated with TIP3P¹⁵ water using a 12Å buffer in a cubic box, using the LEaP module in the AMBER14 software package.¹⁶ Energy minimizations for solvated **1^c**, **7^c**, **8^c** and **9^c** were performed separately under constant volume (500 steps steepest descent, followed by 24500 steps of conjugate-gradient minimization). Each system was subsequently heated to 300K over a period of 50 ps, followed by equilibration at 300K for a further 0.5 ns using the nPT condition, with the Berendsen thermostat¹⁷ for temperature control. All covalent bonds involving hydrogen atoms were constrained using the SHAKE algorithm,¹⁸ allowing a simulation time step of 2 fs throughout the simulation. After equilibration, production simulations were carried out with the GPU implementation¹⁹ of the PMEMD.MPI module, and trajectory frames were collected every 1 ps for a total of 1 μ s. One to four non-bonded interactions were not scaled²⁰ and a non-bonded cut-off of 8 Å was applied to van der Waals interactions, with long-range electrostatics treated with the particle mesh Ewald approximation. Output from each MD simulation was imported into *Prism* (GraphPad) for visualization.

Discussion of Equation [1] For *J*-Coupling Equation Parameterization

The generalized form of the Karplus-like equation that was used to parameterize the dependence of *J*-couplings on a specific torsion angle was first described by Pachler (K. G. R. Pachler, Extended Hückel Theory MO Calculations of Proton-Proton Coupling Constants–II: The Effect of Substituents on Vicinal Couplings in Monosubstituted Ethanes, *Tetrahedron*, **1971**, 27, 187–199). He proposed the use of this trigonometric function to account for asymmetry in the Karplus curve caused by substitution of a hydrogen atom in the coupling pathway. We adopted this trigonometric polynomial form because it provides the best parameterization to the DFT data with the smallest number of terms. This form of the equation is also amenable to simple integration which allowed us to develop the *MA'AT* equation for modeling torsional populations.

Representative Cartesian Coordinates for Structures 1^c, 6^c, 7^c, 8^c and 9^c

Structure 1^c:

C	0.915	0.444	-0.468
C	-0.089	1.564	-0.342
C	-0.827	1.439	0.972
C	-1.459	0.064	1.065
C	-0.432	-1.025	0.763
C	-0.997	-2.440	0.764
O	1.522	0.547	-1.738
O	0.579	2.800	-0.371
O	-1.831	2.422	1.025
O	-1.981	-0.128	2.361
O	-1.787	-2.684	-0.382
O	0.247	-0.799	-0.444
H	1.049	2.876	-1.205
H	-1.413	3.284	0.958
H	-2.373	-0.982	2.419
H	-2.159	-3.568	-0.326
H	1.686	0.494	0.333
H	-0.795	1.556	-1.203
H	-0.138	1.615	1.830
H	-2.308	-0.009	0.335
H	0.329	-0.994	1.585
H	-0.179	-3.196	0.754
H	-1.634	-2.622	1.658
H	3.069	-0.123	-2.901
H	2.408	-1.338	-1.739
H	3.448	0.045	-1.142
C	2.668	-0.265	-1.872

Structure 6^c:

C	5.972	0.406	-0.501
C	4.930	1.494	-0.367
C	4.222	1.350	0.962
C	3.636	-0.044	1.039
C	4.726	-1.077	0.809
O	6.535	0.503	-1.792
O	5.553	2.752	-0.418
O	3.192	2.300	1.057
O	3.060	-0.210	2.311
O	5.356	-0.863	-0.432
H	6.006	2.841	-1.260
H	3.580	3.177	0.987
H	2.433	0.507	2.447
H	6.763	0.501	0.275
H	4.203	1.451	-1.211
H	4.926	1.535	1.806
H	2.820	-0.169	0.290
H	4.287	-2.102	0.788
H	5.491	-1.051	1.617
H	8.083	-0.116	-2.981

H	8.506	0.143	-1.244
C	7.724	-0.242	-1.935
H	7.535	-1.323	-1.753

Structure 7^c:

C	1.044	0.406	-0.483
C	0.040	1.527	-0.357
C	-0.698	1.401	0.957
C	-1.330	0.027	1.050
C	-0.303	-1.062	0.748
C	-0.868	-2.477	0.748
O	1.651	0.510	-1.754
O	0.708	2.763	-0.386
O	-1.702	2.385	1.010
O	-2.409	-0.008	0.147
O	-1.658	-2.721	-0.398
O	0.376	-0.836	-0.459
H	1.178	2.839	-1.220
H	-1.284	3.247	0.943
H	-2.897	0.816	0.250
H	-2.030	-3.605	-0.342
H	1.815	0.456	0.318
H	-0.666	1.519	-1.219
H	-0.009	1.578	1.815
H	-1.766	-0.120	2.067
H	0.458	-1.031	1.570
H	-0.050	-3.233	0.738
H	-1.505	-2.659	1.642
H	3.198	-0.160	-2.916
H	2.537	-1.375	-1.754
H	3.577	0.008	-1.158
C	2.797	-0.302	-1.888

Structure 8^c ($\phi_{(C2'-C1'-O1'-C4)} = 154^\circ$, $\psi_{(C1'-O1'-C4-C3)} = 78^\circ$):

C	-0.346	-1.360	0.660
C	0.178	-2.773	0.396
C	-0.936	-3.768	0.751
C	-1.445	-3.576	2.179
C	-1.835	-2.112	2.347
C	-2.234	-1.767	3.763
C	0.865	3.711	0.227
C	-0.350	3.198	0.978
C	-0.267	1.705	1.282
C	0.214	0.896	0.064
C	1.439	1.568	-0.566
O	0.530	-2.913	-0.974
H	1.155	-2.317	-1.142
O	-0.515	3.965	2.166
H	-0.618	4.705	2.018
O	0.658	-0.425	0.428
O	0.923	0.835	-2.819
H	1.241	0.452	-3.457

O	1.086	2.909	-0.926
H	-1.137	-1.170	0.078
O	-1.581	1.332	1.698
H	0.979	-2.948	0.968
H	-1.791	1.745	2.342
H	-1.703	-3.571	0.141
O	-0.557	-5.118	0.508
H	-2.247	-4.154	2.328
H	-0.356	-5.273	-0.318
H	-2.591	-1.898	1.728
O	-0.431	-3.920	3.115
H	-3.006	-2.323	4.038
H	-1.482	-1.957	4.378
H	-0.670	-4.563	3.522
H	1.671	3.706	0.818
O	-0.712	-1.272	2.035
H	-1.154	3.348	0.402
O	-2.585	-0.383	3.841
H	0.369	1.562	2.041
H	-1.939	0.011	3.622
H	-0.520	0.831	-0.611
O	0.569	5.003	-0.186
H	2.177	1.596	0.109
C	1.941	0.863	-1.817
H	2.737	1.337	-2.167
H	2.210	-0.063	-1.591
C	1.715	5.747	-0.593
H	1.459	6.679	-0.757
H	2.082	5.360	-1.414
H	2.394	5.715	0.114

Structure **9^c** ($\phi_{(C2'-C1'-O1'-C4)} = 156^\circ$, $\psi_{(C1'-O1'-C4-C3)} = 94^\circ$):

C	-0.070	-1.406	-0.069
C	0.789	-2.666	-0.188
C	-0.116	-3.816	-0.651
C	-1.326	-4.001	0.266
C	-2.033	-2.656	0.387
C	-3.177	-2.679	1.375
C	0.461	3.772	0.791
C	-0.848	3.060	1.084
C	-0.678	1.550	1.218
C	0.217	0.970	0.108
C	1.481	1.821	-0.049
O	1.827	-2.460	-1.136
H	2.311	-1.785	-0.846
O	-1.428	3.627	2.254
H	-1.571	4.371	2.172
O	0.692	-0.352	0.425
H	2.060	1.465	-0.928
O	1.089	3.170	-0.333
H	-0.457	-1.165	-0.959
O	-2.003	1.018	1.181
H	1.186	-2.889	0.702

H	-2.433	1.313	1.780
H	-0.471	-3.561	-1.550
O	0.597	-5.035	-0.824
H	-1.950	-4.671	-0.136
H	1.229	-4.980	-1.412
H	-2.377	-2.380	-0.511
O	-0.909	-4.449	1.549
H	-3.846	-3.354	1.097
H	-2.839	-2.930	2.272
H	-1.190	-5.188	1.663
H	1.063	3.742	1.588
O	-1.112	-1.665	0.869
H	-1.469	3.232	0.320
O	-3.788	-1.388	1.434
H	-0.269	1.345	2.107
H	-3.219	-0.895	1.667
H	-0.286	0.950	-0.756
O	0.143	5.084	0.467
H	1.977	1.843	0.820
C	1.262	5.967	0.508
H	0.954	6.890	0.388
H	1.887	5.736	-0.210
H	1.714	5.883	1.374

Complete reference 28

M. J. Frisch, G. W. Trucks, H. B. Schlegel, G. E. Scuseria, M. A. Robb, J. R. Cheeseman, G. Scalmani, V. Barone, G. A. Petersson, H. Nakatsuji, X. Li, M. Caricato, A. V. Marenich, J. Bloino, B. G. Janesko, R. Gomperts, B. Mennucci, H. P. Hratchian, J. V. Ortiz, A. F. Izmaylov, J. L. Sonnenberg, D. Williams-Young, F. Ding, F. Lipparini, F. Egidi, J. Goings, B. Peng, A. Petrone, T. Henderson, D. Ranasinghe, V. G. Zakrzewski, J. Gao, N. Rega, G. Zheng, W. Liang, M. Hada, M. Ehara, K. Toyota, R. Fukuda, J. Hasegawa, M. Ishida, T. Nakajima, Y. Honda, O. Kitao, H. Nakai, T. Vreven, K. Throssell, J. A. Montgomery Jr., J. E. Peralta, F. Ogliaro, M. J. Bearpark, J. J. Heyd, E. N. Brothers, K. N. Kudin, V. N. Staroverov, T. A. Keith, R. Kobayashi, J. Normand, K. Raghavachari, A. P. Rendell, J. C. Burant, S. S. Iyengar, J. Tomasi, M. Cossi, J. M. Millam, M. Klene, C. Adamo, R. Cammi, J. W. Ochterski, R. L. Martin, K. Morokuma, O. Farkas, J. B. Foresman and D. J. Fox, *Gaussian 16*, Revision B.01, Gaussian, Inc., Wallingford, CT, 2016.

Supporting Information References

1. C. A. Podlasek, J. Wu, W. A. Stripe, P. B. Bondo and A. S. Serianni, *J. Am. Chem. Soc.*, 1995, **117**, 8635–8644.
2. P. W. Austin, F. E. Hardy, J. G. Buchanan and J. Baddiley, *J. Chem. Soc.*, 1963, 5350–5353.
3. K. Mereiter, T. Rosenau, B. Adad and P. Kosma, P. , *CSD Comm.*, 2004. REFCODE: XYLOMB02; CCDC 244329.
4. B. Sheldrick, *Acta Cryst.*, 1977, **B33**, 3003–3005.
5. S. Takagi and G. A. Jeffrey, *Acta Cryst.*, 1978, **B34**, 2006–2010.
6. S. Takagi and G. A. Jeffrey, *Acta Cryst.*, 1979, **B35**, 902–906.
7. R. Stenutz, M. Shang and A. S. Serianni, *Acta Cryst.*, 1999, **C55**, 1719–1721.
8. W. Zhang, A.G. Oliver and A. S. Serianni, *Acta Cryst.*, 2012, **C68**, o7–o11.
9. T. Turney, Q. Pan, W. Zhang, A. G. Oliver and A. S. Serianni, *Acta Cryst.*, 2019, **C75**, 161–167.
10. W. Zhang, M.-K. Yoon, R. J. Meredith, J. Zajicek, A. G. Oliver, M. Hadad, M. H. Frey, I. Carmichael and A. S. Serianni, *Phys. Chem. Chem. Phys.*, 2019, **21**, 23576–23588.
11. P. Thureau, I. Carvin, F. Ziarelli, S. Viel and G. Mollica, *Angew. Chem.*, 2019, **131**, 16193–16197.
12. P. Thureau, G. Mollica, F. Ziarelli and S. Viel, *J. Magn. Reson.*, 2013, **231**, 90–94.
13. Complex Carbohydrate Research Center (CRCC), University of Georgia.
<http://www.glycam.org>

14. K. N. Kirschner; A. B. Yongye, S. M. Tschampel, J. González-Outeiriño, C. R. Daniels, B. L. Foley and R. J. Woods, *J. Comput. Chem.*, 2008, **29**, 622–655.
15. W. L. Jorgensen, J. Chandrasekhar, J. D. Madura, R. W. Impey and M. L. Klein, *J. Chem. Phys.* 1983, **79**, 926–935.
16. D. A. Case, V. Babin, J. T. Berryman, R. M. Betz, Q. Cai, D. S. Cerutti, T. E. I. Cheatham, T. A. Darden, R. E. Duke, H. Gohlke, *et al.* AMBER 14, 2014, University of California, San Francisco.
17. H. J. C. Berendsen, J. P. M. Postma, W. F. van Gunsteren, A. DiNola and J. R. Haak, *J. Chem. Phys.*, 1984, **81**, 3684–3690.
18. W. F. van Gunsteren and H. J. C. Berendsen, *Mol. Phys.*, 1977, **34**, 1311–1327.
19. A. W. Götz, M. J. Williamson, D. Xu, D. Poole, S. Le Grand and R. C. Walker, *J. Chem. Theory Comput.*, 2012, **8**, 1542–1555.
20. K. N. Kirschner and R. J. ; Woods, *Proc. Natl. Acad. Sci. U. S. A.*, 2001, **98**, 10541–10545.